



## RESEARCH ARTICLE

# Preferential binding of ADP-bound mitochondrial HSP70 to the nucleotide exchange factor GRPEL1 over GRPEL2

Pooja Manjunath<sup>1</sup>  | Gorazd Stojkovič<sup>2</sup>  | Liliya Euro<sup>1</sup> |  
Svetlana Konovalova<sup>3</sup> | Sjoerd Wanrooij<sup>2</sup> | Kristian Koski<sup>4</sup> | Henna Tyynismaa<sup>1</sup>

<sup>1</sup>Stem Cells and Metabolism Research Program, Faculty of Medicine, University of Helsinki, Helsinki, Finland

<sup>2</sup>Department of Medical Biochemistry and Biophysics, Umeå University, Umeå, Sweden

<sup>3</sup>Institute of Biotechnology, University of Helsinki, Helsinki, Finland

<sup>4</sup>Biocenter Oulu and Faculty of Biochemistry and Molecular Medicine, University of Oulu, Oulu, Finland

## Correspondence

Pooja Manjunath, Stem Cells and Metabolism Research Program, Faculty of Medicine, University of Helsinki, Haartmaninkatu 8, 00014 Helsinki, Finland.

Email: [pooja.manjunath@helsinki.fi](mailto:pooja.manjunath@helsinki.fi)

## Present addresses

Gorazd Stojkovič and Sjoerd Wanrooij, University Hospital of Umeå, Umeå, Sweden.

## Funding information

Orionin Tutkimussäätiö; Sigrid Juséliuksen Säätiö; Academy of Finland

**Review Editor:** Zengyi Chang

## Abstract

Human nucleotide exchange factors GRPEL1 and GRPEL2 play pivotal roles in the ADP–ATP exchange within the protein folding cycle of mitochondrial HSP70 (mtHSP70), a crucial chaperone facilitating protein import into the mitochondrial matrix. Studies in human cells and mice have indicated that while GRPEL1 serves as an essential co-chaperone for mtHSP70, GRPEL2 has a role regulated by stress. However, the precise structural and biochemical mechanisms underlying the distinct functions of the GRPEL proteins have remained elusive. In our study, we present evidence revealing that ADP-bound mtHSP70 exhibits remarkably higher affinity for GRPEL1 compared to GRPEL2, with the latter experiencing a notable decrease in affinity upon ADP binding. Additionally, Pi assay showed that GRPEL1, but not GRPEL2, enhanced the ATPase activity of mtHSP70. Utilizing AlphaFold modeling, we propose that the interaction between GRPEL1 and mtHSP70 can induce the opening of the nucleotide binding cleft of the chaperone, thereby facilitating the release of ADP, whereas GRPEL2 lacks this capability. Additionally, our findings suggest that the redox-regulated Cys87 residue in GRPEL2 does not play a role in dimerization but rather reduces its affinity for mtHSP70. Our findings on the structural and functional disparities between GRPEL1 and GRPEL2 may have implications for mitochondrial protein folding and import processes under varying cellular conditions.

## KEYWORDS

AlphaFold, co-chaperone, cysteines, GRPEL1, GRPEL2, interactions, mitochondria, mtHSP70, nucleotide exchange factor

## 1 | INTRODUCTION

Mitochondria are major metabolic regulator organelles that import most of their proteome from the cytosol. The

molecular chaperone mtHSP70 of the (heat shock protein) HSP70 family plays a specialized role in the translocation of preproteins into the mitochondrial matrix and in their proper folding (Bracher & Verghese, 2023; Kang

This is an open access article under the terms of the [Creative Commons Attribution-NonCommercial-NoDerivs](https://creativecommons.org/licenses/by-nc-nd/4.0/) License, which permits use and distribution in any medium, provided the original work is properly cited, the use is non-commercial and no modifications or adaptations are made.

© 2024 The Author(s). *Protein Science* published by Wiley Periodicals LLC on behalf of The Protein Society.

et al., 1990). Its protein binding/release cycle is regulated by co-chaperones, which for the bacterial Hsp70 homologue DnaK were identified as DnaJ and the nucleotide exchange factor (NEF) GrpE (Hosfelt et al., 2022; Liberek et al., 1991). ATP hydrolysis by DnaJ stabilizes the interaction of substrate protein with DnaK, whereas GrpE triggers ADP to ATP exchange, accelerating substrate release, which is rate-limiting in the cycle (Szabo et al., 1994; Xiao et al., 2024). Prokaryotic and eukaryotic Hsp70 systems are functionally similar; however, in eukaryotes, a GrpE-like NEF is found only in mitochondria (Harrison, 2003). The most studied mitochondrial NEF is Mge1, the sole GrpE-like protein in *Saccharomyces cerevisiae*, which is essential for viability (Bolliger et al., 1994; Krzewska et al., 2001; Laloraya et al., 1994). Interestingly, two distinct GrpE-like mitochondrial proteins exist in mammals, GRPEL1 and GRPEL2 (Goswami et al., 2010; Naylor et al., 1996; Naylor et al., 1998; Srivastava et al., 2017), but the structural attributes to their function are not well known.

Bacterial GrpE and yeast Mge1 interact with their respective chaperones as dimers (Harrison et al., 1997; Moro & Muga, 2006; Wu et al., 2012). Notably, human GRPEL1 and GRPEL2 are functionally homodimers (Konovalova et al., 2018) but their stoichiometric interaction with mtHSP70 is yet to be addressed. High-resolution structural information is available only for bacterial GrpE (Harrison et al., 1997; Nakamura et al., 2010; Wu et al., 2012; Xiao et al., 2024). Analysis of the GrpE G122D-DnaK complexes from *Escherichia coli* (PDB-ID1DKG) and *Mycobacterium tuberculosis* (PDB-ID 8GB3) revealed a 2:1 stoichiometry, characterized by an asymmetric interaction between one of the monomers of GrpE dimer and DnaK (Harrison et al., 1997; Xiao et al., 2024). Conversely, when structurally analyzed, the *Geobacillus kaustophilus* GrpE homodimer bound to DnaK exhibited a 2:2 stoichiometry (PDB-ID 4ANI), where each GrpE monomer interacted with its corresponding DnaK monomer, leading to a stiffer dimeric GrpE structure (Wu et al., 2012). While interaction diversity exists among NEFs, the primary function is consistent: binding to the ADP-bound nucleotide-binding domain (NBD) of the chaperones to facilitate ADP release (Bracher & Verghese, 2023). Recent studies show that the interaction of GrpE with DnaK serves to allosterically regulate the chaperone, leading to the release of ADP as well as the folded protein from the substrate binding domain (SBD) (Rossi et al., 2024; Xiao et al., 2024).

GRPEL1 is conserved across all metazoans, whereas GRPEL2 is found in vertebrates, and both have ubiquitous expression in human tissues (Konovalova et al., 2018; Naylor et al., 1998). However, evidence now indicates that GRPEL1, but not GRPEL2, is the essential housekeeping

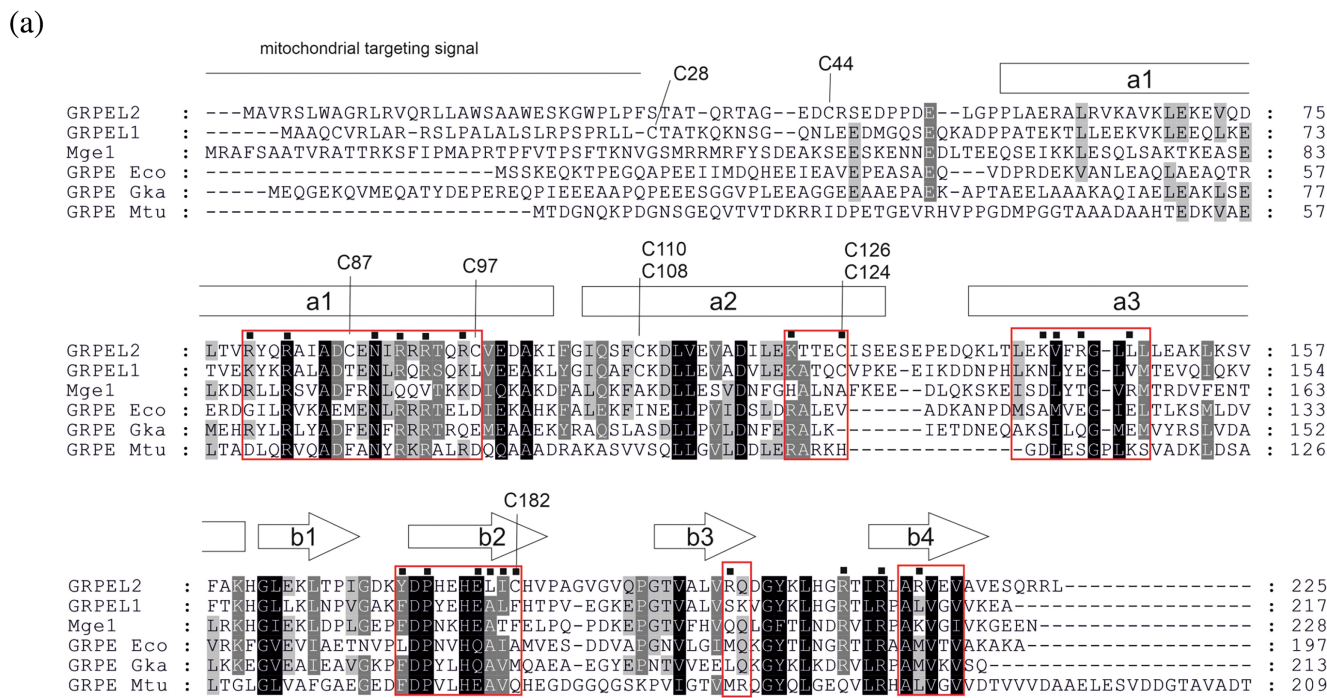
NEF for mtHsp70 in mammalian cells: (i) Only human GRPEL1 was able to complement yeast Mge1 (Srivastava et al., 2017). (ii) Mitochondrial protein import was not impaired in human GRPEL2 knockout cells (Konovalova et al., 2018). (iii) Human variation data indicates that the GRPEL1 gene is not tolerant to loss-of-function variants, unlike GRPEL2 (Konovalova et al., 2018). (iv) Mouse knockout of GRPEL1 was lethal in early development, and the depletion of GRPEL1 in skeletal muscles of adult mice led to severe muscle atrophy and premature death, showing that GRPEL2 was not able to compensate for GRPEL1 loss (Neupane et al., 2022). In contrast, we previously reported that GRPEL2 may play a specific role in stress sensing similar to Mge1, which is an oxidative stress sensor in yeast (Marada et al., 2013). We observed that in cultured human cells, the dimerization of GRPEL2 increased under oxidative stress and was dependent on redox-regulated Cys87 (Konovalova et al., 2018). In agreement, a competitive cysteine-reactive profiling study recently identified Cys87 as the most redox-sensitive cysteine of GRPEL2 (Kisty et al., 2023).

In this study, we aimed to explicate the fundamental structural, biochemical, and biophysical differences between GRPEL1 and GRPEL2 to increase our understanding of their potential roles. In our investigation, we revealed an enhanced interaction specifically between ADP-bound mtHSP70 and GRPEL1. Furthermore, we show that disulfide affects the stability of GRPEL2 and impedes its interaction with mtHSP70. These findings further strengthen the importance of GRPEL1 as the main NEF for mtHSP70 in human mitochondria.

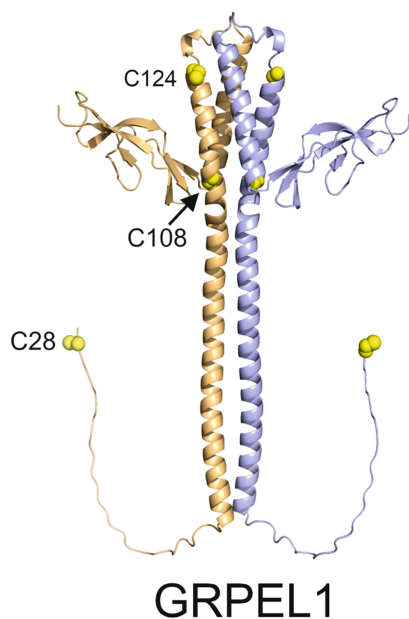
## 2 | RESULTS

### 2.1 | Sequence comparison of the GRPELs highlights the unique cystines in GRPEL2

To explore the distinctions in interactions between mtHSP70 and both GRPELs, we examined the amino acid sequence variances among the NEFs and compared them with yeast Mge1 and three bacterial GrpE sequences (*G. kaustophilus*, *E. coli*, and *M. tuberculosis*) (Figure 1a). We further studied the cysteine pattern and structure of the GRPELs by calculating the dimeric models with the help of AlphaFold 2 (Jumper et al., 2021) (Figure 1b,c). In GRPEL2, Cys87, the most redox-sensitive cysteine (Kisty et al., 2023), locates in the middle of the long  $\alpha$ 1-helix, and the dimeric AlphaFold2 model proposes that it forms a disulfide bridge with the corresponding cysteine of the dimer partner (Figure 1c). As seen in the sequence alignment of the GrpE family of proteins (Figure 1a), Cys87 is



(b)



(c)

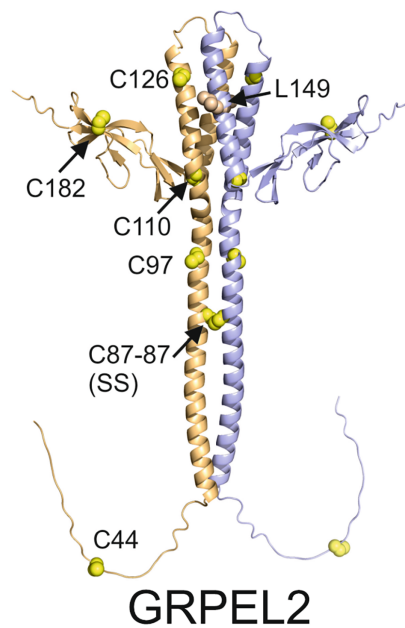


**FIGURE 1** Sequence comparison of the GRPELs highlights the unique cysteines in GRPEL2. (a) Sequence alignment of GrpE protein family members including GRPEL1 and GRPEL2, the yeast Mge1, and the three bacterial GrpE proteins from *E. coli*, *G. kaustophilus*, and *M. tuberculosis*, which have crystal structures and Cryo-EM structures determined (PDB codes 4ANI, (GrpE-G122D)1DKG and 8GB3, respectively). The cysteines in GRPEL2 and GRPEL1 are highlighted and labeled. The secondary structure elements of GRPEL2 are shown above the sequences as predicted by the AlphaFold2 model. The regions that are shown to interact with HSP70 by structural GrpE studies (Harrison et al., 1997) (Wu et al., 2012) and by the modeling studies of this study (by AlphaFold2 Multimer, see Figure S1) are shown with boxes around the sequence regions. Some key residues forming the interactions are highlighted with black squares. Met155 is a critical redox sensor in Mge1 (Marada et al., 2013). The corresponding Leu149 of GRPEL2 is highlighted with an arrow. (b) AlphaFold2 model of the GRPEL1 dimer as calculated using AlphaFold2 Colab (Evans et al., 2021; Jumper et al., 2021). The chains are colored as light orange and blue. The cysteine residues are shown with yellow spheres. (c) AlphaFold2 model of the GRPEL2 dimer. The coloring scheme is the same as in panel (b). All the cysteines, and the Leu149, corresponding to Met155 of Mge1, are shown with light brown spheres. GRPEL models exclude the mitochondrial targeting signal in the N-terminus of both chains.

only found in GRPEL2. Similarly, the next cysteine, Cys97, located in the  $\alpha$ 1-helix, is only present in GRPEL2. However, Cys97 is not forming a disulfide bridge according to the AlphaFold2 model but points to the bulk solvent. The next two cysteines, Cys110 and Cys126, both located in the  $\alpha$ 2-helix, are found in GRPEL1 and GRPEL2, but are not conserved in yeast or bacterial homologues (Figure 1a). These two cysteines have also been shown to possess redox-sensitivity properties (Kisty et al., 2023). GRPEL2 has an additional unique cysteine at the end of  $\beta$ 2 (Cys182). Both GRPEL1 and GRPEL2 have one N-terminal cysteine (C28 and C44, respectively) in the random-coil region. These sequence comparisons suggest that unique cysteines in GRPEL2 may perform specific roles under stress conditions.

## 2.2 | Purified-soluble human GRPELs exist in dimeric form and cysteines have no role in oligomerization

To investigate the biophysical and biochemical differences between GRPELs, we purified recombinant human GRPEL1, GRPEL2, and mtHSP70 as well as mutant variants of GRPEL2 with either a Cys87 to Ala (GRPEL2-C87A) or a Cys97 to Ala (GRPEL2-C97A). The mtHSP70 and GRPEL constructs were purified by affinity chromatography and size-exclusion chromatography (SEC). All the protein obtained was soluble, and the concentrations were typically between 4 and 8 mg/mL. After the purification step, the

purified GRPEL proteins resulted in a single protein band with a molecular mass of around 25 kDa in SDS-PAGE while the purified mtHSP70 exhibited greater heterogeneity, with the primary band aligning with a size of around 70 kDa (Figure 2a). However, the gel filtration profile displayed several peaks corresponding to different elution volumes for all GRPELs, indicating heterogeneity in the oligomerization state of the protein (Figure S1a–d). The major peaks, eluted at approximately 13 mL in the 24 mL SEC column, were collected and concentrated. To analyze differences between GRPEL2 and its mutants, we conducted reduced and non-reducing SDS-PAGE followed by immunoblotting. This revealed distinct bands corresponding to several molecular masses for all GRPEL2 proteins. In addition, we observed differences in oligomerization between GRPEL2-C87A and wild-type GRPEL2, but not between GRPEL2-C97A and wild-type (Figure 2b). These observations imply the dynamic nature of GRPELs and their ability to exist in a multi-oligomeric state while maintaining solubility in solution.

## 2.3 | Structural stability of GRPELs depends on the interactions of cysteines

We aimed to understand the role of cysteines in the stability of GRPELs using circular dichroism (CD) spectrophotometry. We compared the CD spectrums of wild-type GRPEL1 and GRPEL2 with those of mutant GRPEL2-C87A and

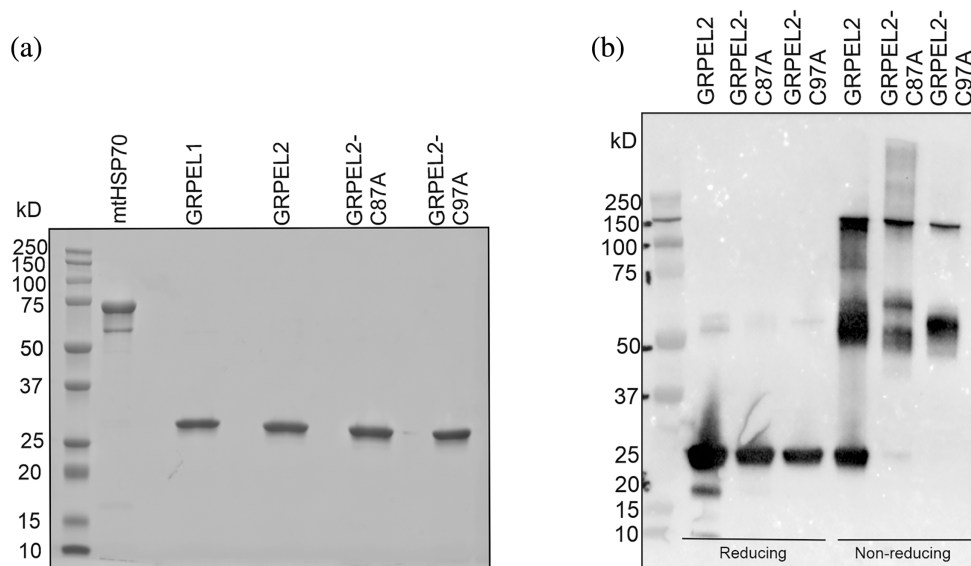


**FIGURE 2** Purified-soluble human GRPELs exist in higher oligomeric forms. (a) Proteins treated with beta-mercaptoethanol and subjected to a 10 min boiling step, then run in a 10% SDS gel, show mtHSP70 at 70 kDa, and GRPEL1, GRPEL2, GRPEL2-C87A, and GRPEL2-C97A at 25 kDa. (b) Western blot of GRPEL2, GRPEL2-C87A, and GRPEL2-97A, in reducing and non-reducing conditions. The non-reducing samples, GRPEL2-C87A show difference in oligomerization compared to wild type GRPEL2 and C97A, showing the effect of C87 in oligomer formation.

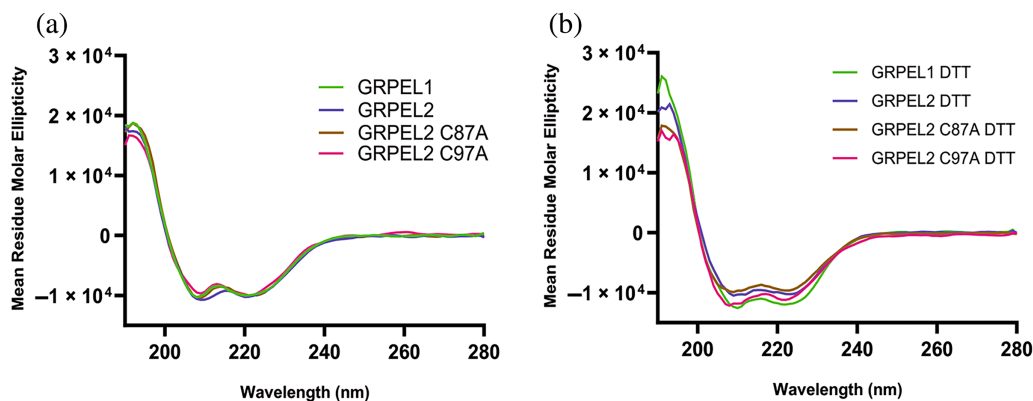


**FIGURE 3** Structural stability of GRPELs depends on the interactions of cysteines. (a) GRPEL1, GRPEL2, GRPEL2-C87A, and GRPEL2-C97A represent samples diluted with buffer under nonreducing conditions. (b) GRPEL1, GRPEL2, GRPEL2-C87A, and GRPEL2-C97A represent samples diluted with buffer and the curves diluted with buffer with 1 mM DTT. Here, significant differences were detected with or without DTT in GRPEL1, GRPEL2-C87A, and GRPEL2-C97A but not in GRPEL2. GRPEL2 and GRPEL2-C87A have identical CD curves in the buffer with DTT, indicating the role of Cys87 in maintaining the protein conformation.

GRPEL2-C97A (Figure 3 and Figure S2). The far UV CD spectra measurement at 180–280 nm indicated that the recombinant proteins were folded and soluble. In the far-UV spectrum, all the recombinant GRPEL proteins were mostly  $\alpha$ -helical (31%–38%) with a smaller number of  $\beta$ -sheet structures (Table 1). Proteins with and without DTT in the buffer were compared, where DTT was used to reduce all the cysteines (Figure 3). In the absence of DTT, we noticed differences in the CD curves between GRPEL2 and GRPEL2-C87A. However, when we added DTT, these differences disappeared. At the same time, adding DTT caused notable changes in the CD spectra of GRPEL1, GRPEL2-C87A, and GRPEL2-C97A compared to their respective non-reducing forms (Figure S2a,b,e–h), but there were no changes in the CD profile of GRPEL2 (Figure S2c,d). Comparing the statistically significant differences in secondary structures revealed that most of those changes occurred in the alpha-helix and antiparallel regions (Figure S2b,f,h).

When comparing the thermal stability of proteins in buffers without DTT, GRPEL1 demonstrated higher thermal stability than GRPEL2, with a melting temperature approximately 9°C higher (Figure 4a,b). This finding aligns with previous research (Borges et al., 2003; Oliveira et al., 2006). Mutants GRPEL2-C87A and GRPEL2-C97A exhibited even higher melting temperatures, indicating greater thermo-stability compared to wild type GRPEL2 (Figure 4c,d). In the presence of DTT, GRPEL1 showed improved thermal stability compared to its state without DTT, while no marked change was observed for GRPEL2 (Figure 4e,f). Mutants GRPEL2-C87A and GRPEL2-C97A in the DTT buffer displayed stability similar to that of wild-type GRPEL2 (Figure 4g,h). In conclusion, the comparison of wild-type GRPEL2 with its mutants' spectral

analysis and thermal stability profiles suggests that the presence of Cys87 and Cys97 in GRPEL2 contributes to its reduced stability.

## 2.4 | Multiangle light scattering reveals that only GRPEL1 forms a complex with mtHSP70

We characterized purified mtHSP70, GRPEL1, GRPEL2, and GRPEL2 mutants along with their possible complexes using size-exclusion chromatography coupled with multi-angle light scattering (SEC-MALS). This method reliably determined the absolute molecular weight of proteins or complexes without additional standard proteins. Wild-type GRPELs displayed two distinct peaks (Figure S3a,b) with the major peak corresponding to dimeric forms at 13 mL and the minor peak eluting at around 11.5 mL (Figure 5a and Figure S3). The determined molecular weights (based on three separate runs averaged, Table 2) for major peak protein were 52.5/55.72 kDa and for minor peak protein 111 kDa, corresponding to dimeric and tetrameric forms of GRPELs, respectively (theoretical MWs of dimeric and tetrameric GRPEL1 and GRPEL2 are 52.17/54.47 and 104.34/108.94 kDa, respectively). Addition of 1 mM DTT reduced aggregated protein levels but did not alter GRPEL2 elution volumes or the determined molecular weights (Figure S3e and Table 3). Most mtHSP70 eluted as monomeric protein at 13.7 mL with the determined MW of 70.3 kDa (Table 2). A minor fraction was also present in the SEC-MALS analysis showing higher oligomers (166 kDa). GRPEL2-C87A and GRPEL2-C97A variants exhibited SEC profiles similar to wild type GRPEL2 (Figure S3c,d), and the determined MWs were similar to

TABLE 1 CD measurements and  $T_m$  values for various GRPELs in both the non-reducing buffer and a buffer containing DTT.

	GRPEL1	GRPEL1 + DTT	GRPEL2	GRPEL2 + DTT	GRPEL2-C87A	GRPEL2-C87A + DTT	GRPEL2-C97A	GRPEL2-C97A + DTT
Helix (%)	32.50	38.30	36.50	34.60	35.60	35.10	31.10	34.40
Antiparallel (%)	9.70	5.80	7.10	8.10	7.30	8.10	11.10	9.00
Parallel (%)	8.40	7.30	7.60	8.00	7.90	7.80	8.70	7.80
Beta-Turn (%)	17.20	16.10	16.50	16.80	16.60	16.80	17.50	17.10
Rndm. coil (%)	31.30	27.70	28.30	30.00	29.80	28.80	32.20	28.60
Total sum (%)	99.10	95.30	96.00	97.50	97.10	96.70	100.60	96.90
$T_m$ (°C)	55.2 ± 0.2	58.3 ± 0.2	46.5 ± 0.2	46.3 ± 0.4	48.6 ± 0.2	45.8 ± 0.2	52.1 ± 0.8	45.6 ± 0.6

Note: Comparing  $T_m$  between GRPEL1 and GRPEL1 DTT shows increased stability in reduced proteins. Conversely, GRPEL2 samples display no significant change in  $T_m$  values. Mutants GRPEL2 C87A and C97A exhibit higher  $T_m$  values than the wild type; however, all reduced mutants show similar  $T_m$  values to wild-type GRPEL2. All GRPELs display a higher percentage of alpha helix, followed by beta sheet.

wild type GRPELs (Table 2), indicating predominantly dimeric and tetrameric forms that were unaffected by reducing agents, suggesting non-essential roles for cysteines in the coiled-coiled region for dimerization. The possible heterocomplexes of GRPELs with mtHSP70 were studied with SEC-MALS. GRPEL1 or GRPEL2 proteins were mixed with mtHSP70 protein in ratios of 1:1 or 3:1. In the experiments with 1:1 ratio, the SEC profiles resembled the mtHSP70 SEC profile. However, when excess GRPEL1 was used, two additional peaks appeared in the SEC profile (Figure 5a and Figure S4a,c), indicating complex formation. The sizes of these complexes were 107 kDa (major peak, eluted in 12.2 mL) and ~199 kDa (minor peak, eluted in 10.6 mL). These results suggest that 2:1 and 2:2 GRPEL1 and mtHSP70 complexes were formed (expected MWs of 123 and 197 kDa, respectively). In the case of GRPEL2, no complex formation with mtHSP70 was detected (Figure 5b and Figure S4b,d). Both the dimeric form of GRPEL2 and the monomeric form of mtHSP70 eluted at the same peak. The addition of ADP and DTT to the running buffer did not significantly alter the SEC profiles. However, the presence of DTT reduced the amount of aggregated protein. The SEC-MALS findings decisively demonstrate the exclusive formation of a visible complex between GRPEL1 and mtHSP70, starkly contrasting with the absence of such interaction with GRPEL2 or its mutants.

## 2.5 | mtHSP70 has partiality to GRPEL1 over GRPEL2 in ADP-bound state

To investigate the direct binding and affinity of the isolated proteins, we used purified mtHSP70, GRPEL1, GRPEL2, GRPEL2-C87A, and GRPEL2-C97A in both reducing and non-reducing conditions and analyzed their interaction with mtHSP70 using microscale thermophoresis (MST). In our investigation, we studied the binding of GRPEL1 and GRPEL2 with mtHSP70, in both the presence and absence of DTT and ADP. We observed that mtHSP70 bound to GRPEL1 (DTT) with a  $K_D$  of 104 nM (Figure 6a) in the absence of ADP and 13.4 nM in its presence (Figure 6b). Conversely, GRPEL2 (DTT) exhibited similar affinity, binding to mtHSP70 with a  $K_D$  of 152 nM without ADP (Figure 6c) and much lower affinity with a  $K_D$  of 942 nM with ADP (Figure 6d) (Table 3). Thus, the presence of ADP improved the affinity between GRPEL1 and mtHSP70 while the opposite impact was observed for GRPEL2, showing ADP binding to the chaperone regulates its NEF preference.

Finally, in the non-reduced conditions, mtHSP70 bound to GRPEL1 with a  $K_D$  of 370 nM and GRPEL2

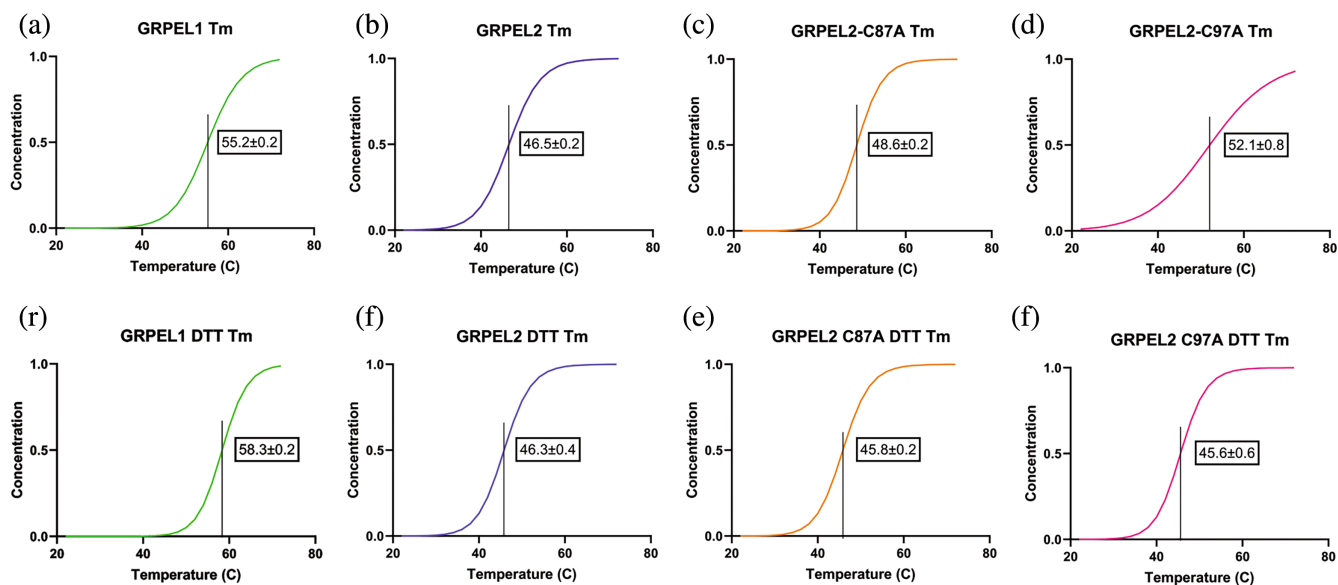


**FIGURE 4** The melting temperature shows the improved stability of reduced GRPEL1. Melting temperatures in non-reducing conditions (a) GRPEL1, (b) GRPEL2, (c) GRPEL2-C87A, and (d) GRPEL2 C97A. The melting temperatures of the same proteins in the presence of reducing agents are represented in (e–h).

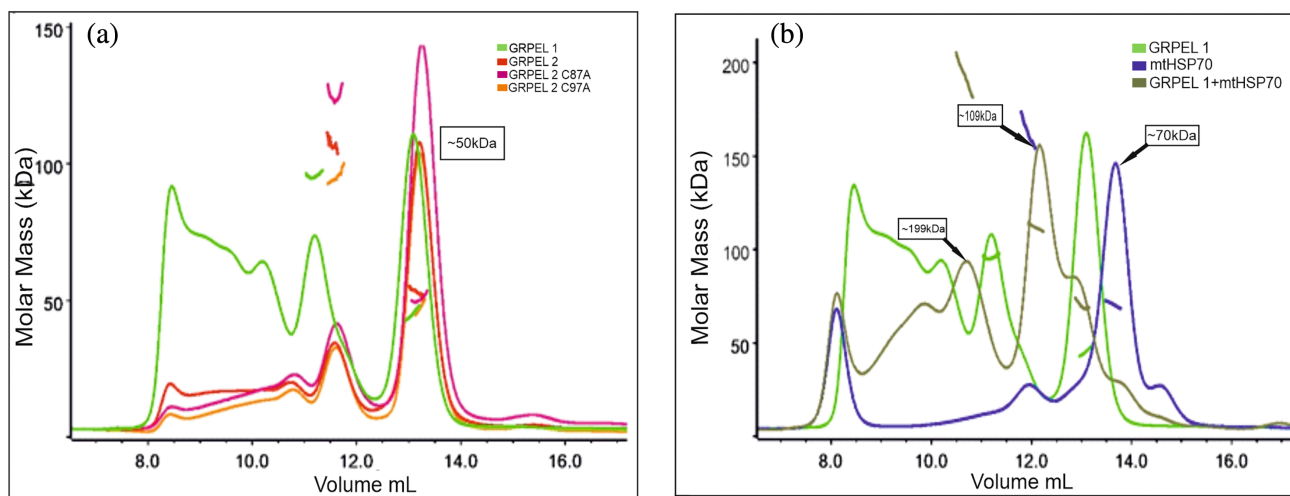


**FIGURE 5** Multiangle light scattering reveals that only GRPEL1 forms a complex with ADP-bound mtHSP70. The SEC-MALS analyses of GRPELs and mtHSP70 and their potential complex. (a) The light scattering signals (angle = 90°) of GRPEL1 (green), GRPEL2 (red), GRPEL2 C87A (magenta), and GRPEL2 C97A (orange) are shown (as eluted from the Superdex200 10/300GL Increase column (GE Healthcare)). In addition, the molecular mass distribution profiles of each run are shown for the peak regions (horizontal lines). The majority of each eluted GRPEL variant eluted in 13 mL as dimers with calculated molecular mass of around 50 kDa. (b) The SEC-MALS results of mtHSP70 alone (blue), GRPEL1 (green), and the complex formed between them (brown). The mtHSP70 eluted in 13.7 mL with calculated molecular mass of 70 kDa indicating monomeric nature of the protein. Interestingly, the elution volume of mtHSP70 was later than that of the dimeric GRPEL1 being smaller in the molecular weight (~50 kDa). Mass distribution is represented by smaller line with respective colors.

with a  $K_D$  of 373 nM (Figures S6a and S5b). These results show that both GRPELs have better affinity in the reduced form in comparison with non-reduced conditions. In the same non-reducing conditions, the mutant GRPEL2-C97A bound with a  $K_D$  457 nM.

Interestingly, GRPEL2-C87A had a better interaction with mtHSP70 (with  $K_D$  203 nM) than GRPEL1, suggesting that the disulfide bond may reduce the interaction of GRPEL2 with mtHSP70 (Figure S5c,d and Table 4).

**TABLE 2** The molecular weights averaged from three separate SEC-MALS runs of mtHSP70, GRPEL1, GRPEL2, GRPEL2-C87A, GRPEL2-C97A, and GREPL2 DTT.

	<b>Major peak kDa</b>	<b>Minor peak kDa</b>	<b>Theoretical MW kDa (monomer)</b>	<b>Theoretical MW kDa (dimer)</b>	<b>Theoretical MW kDa (tetramer)</b>
mtHSP70	<b>73.3</b>	<b>140</b>	74.6	149.46	-
GRPEL1	<b>51.8</b>	<b>98.2</b>	26.1	52.17	104.34
GRPEL2	<b>52.7</b>	<b>101.5</b>	27.24	54.48	108.94
GRPEL2 C87A	<b>50.1</b>	<b>115.6</b>	27.24	54.48	108.94
GRPEL2 C97A	<b>50.5</b>	<b>83.8</b>	27.24	54.48	108.94
GRPEL2 DTT	<b>53.9</b>	<b>99.0</b>	27.24	54.48	108.94

Note: Both UV and IR readings are considered for this calculation. The theoretical molecular weights of the monomer, dimer, and tetramer forms have been calculated using the full-length protein sequences of all GRPELs and mtHSP70, including the 6HIS and TEV cleavage site. Bold represents the emphasis on the obtained experimental value which are crucial results.

<b>ADP</b>	<b>+ GRPEL1</b>	<b>+ GRPEL2</b>	<b>- GRPEL1</b>	<b>- GRPEL2</b>
Bound	957.83	907.31	951.7	970.34
Unbound	941.68	893.35	936.4	927.19
Kd (nM)	<b>13.4</b>	<b>942</b>	<b>104</b>	<b>152</b>
Target conc (nM)	10	10	10	10
Standard deviation:	1.14	2.45	1.05	1.76
Kd confidence:	$\pm 3.5E-09$	$\pm 7.4E-07$	$\pm 2.3E-08$	$\pm 2.3E-08$

Note: The results demonstrate a significant difference in affinity between GRPEL1 and GRPEL2 with ADP-bound mtHSP70, whereas there is no change in affinity between GRPELs and mtHSP70 in the absence of ADP. Bold represents the emphasis on the obtained experimental value which are crucial results.

**TABLE 3** MST Fit Information for the interaction between mtHSP70 (target) with or without ADP bound and the ligands GRPEL1 and GRPEL2 under reducing conditions.

## 2.6 | GRPEL1 facilitates ADP-to-ATP exchange, enhancing the ATP hydrolysis of mtHSP70

To evaluate the NEF activity of GRPELs, we measured the total inorganic phosphate (Pi) released during ATP hydrolysis by mtHSP70. The full-length mtHSP70 exhibits slow intrinsic ATP hydrolysis activity (Zhai et al., 2008). The rate of ATP consumption by mtHSP70 depends on its ability to hydrolyze ATP and efficiently exchange ADP for ATP at its active site. NEFs stimulate this nucleotide exchange, resulting in increased ATP hydrolysis and faster accumulation of Pi over time. In our phosphorylase assay, we first established a baseline by measuring Pi accumulation by mtHSP70 alone. We then compared this baseline with reactions containing either GRPEL1 or GRPEL2. We found that the addition of GRPEL1 significantly enhanced ATP hydrolysis by mtHSP70, while the presence of GRPEL2 produced a similar effect to mtHSP70 alone (Figure 7a). Over time (1, 2, and 2.5 h), Pi accumulation increased gradually in all reactions but it was significantly higher in the presence of GRPEL1 in comparison to either baseline or the

presence of GRPEL2 (Figure 7a). Notably, there was a substantial increase in Pi accumulation between 2 and 2.5 h in both the baseline and GRPEL1-containing reactions. Although Pi levels also rose in the GRPEL2-containing reaction during this interval, the amount of Pi at 2.5 h remained similar to baseline. Further, we also performed an ATPase assay using radiolabeled ATP. The analysis of exchange with cold ATP rendered exchange only with GRPEL1 but not with GRPEL2 or its mutants (Figure 7b). These results demonstrate that GRPEL1 effectively exhibits NEF activity by promoting the exchange of ADP for ATP at the active site of mtHSP70, thereby enhancing further ATP hydrolysis.

## 2.7 | GRPEL1 facilitates cleft opening for ADP release from the mtHSP70 nucleotide binding domain, contrasting with GRPEL2

To investigate the interaction patterns between GRPELs and mtHSP70, we utilized AlphaFold-multimer to model human GRPELs with mtHSP70 with 2:1 and 2:2 stoichiometry. In the complexes, the full-length mtHSP70 takes



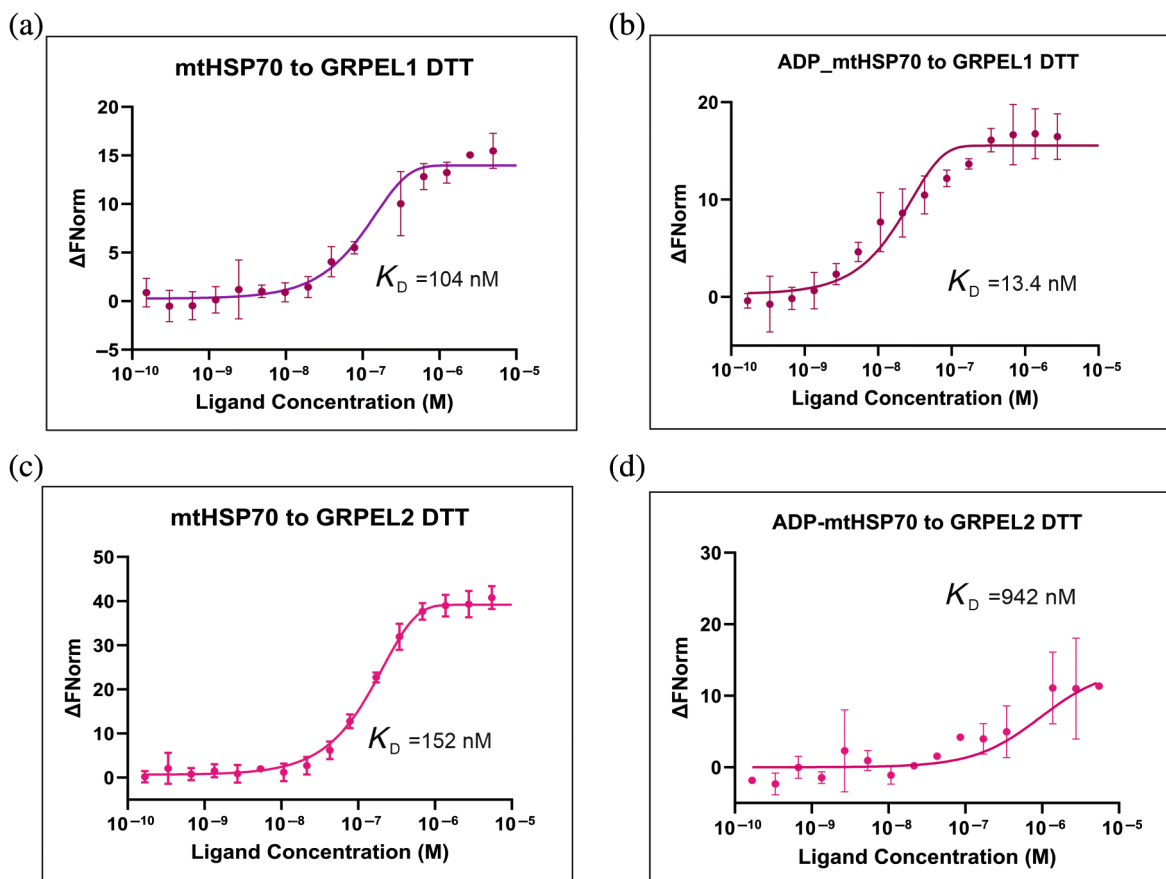


**FIGURE 6** GRPEL1 predominantly binds to ADP-mtHSP70 with high binding affinity. The MST curve represents the binding of the ligand (a) GRPEL1 to mtHSP70 in presence of DTT, showing an affinity of  $K_D = 104$  nM and (b) GRPEL1 to ADP-mtHSP70, showing an affinity of  $K_D = 13.4$  nM. While (c) GRPEL2 to mtHSP70 in presence of DTT  $K_D = 152$  nM and (d) GRPEL2 to ADP-mtHSP70 with affinity of  $K_D = 942$  nM. Here, the binding affinity varies between both proteins, showing preference for GRPEL1 over GRPEL2. The mean ( $\pm$ SD) was calculated from  $n = 3$  based on three independent experiments.

an unexpected conformation, which resembles the ATP-bound state of the chaperone (Figure S6a,b). Because in this study we were mostly interested in the interactions between GRPELs and the NBD of mtHSP70, the calculations were done accordingly by following the approach outlined by Rossi et al. (Evans et al., 2021; Jumper et al., 2021; Rossi et al., 2024) (Figure 8). The modeled complex structures suggest that both human GRPELs predominantly interact with the NBD via the middle portion of the coiled-coil region (residues Lys79–Leu97) and the C-terminal  $\beta$ -sheet domain, including beta strands 2, 3, and 4 (see alignment in Figure 1, Figure 8a,b, and Figure S6a,b). In the complex structure of GRPEL1 and NBD, also the  $\alpha$ -helices  $\alpha_2$  and  $\alpha_3$  of the four-helical bundle are forming interactions with the IIB region of NBD (Figure 8). This interaction is critical to induce the opening of the nucleotide-binding pocket as seen in the modeled *E. coli* GrpE-NBD complex and in the cryo-EM structure of the *M. tuberculosis* GrpE-DnaK complex (Figure 8c). In bacteria, this cleft opening facilitates the

release of the bound ADP molecule from NBD. In the model of human GRPEL2 and NBD, similar interactions with the region IIB of NBD and the  $\alpha$ -helical bundle region of GRPEL2 did not form, leaving the nucleotide-binding pocket in closed conformation (Figure 8b). This conformation resembles the GrpE-DnaK crystal structure of *E. coli*, where a point mutation (G122D) in the four-helical bundle of GrpE hindered the activation of the IIB region of NBD (Grimshaw et al., 2005; Harrison et al., 1997) (Figure S7). Therefore, our modeling studies suggest that GRPEL1's interaction with mtHSP70 NBD resembles a functional NEF interaction, while GRPEL2 does not support the opening of the nucleotide-binding pocket and the following ADP release and NEF function.

### 3 | DISCUSSION

Mitochondrial protein balance plays a crucial role in cellular health and metabolism. To maintain proteostasis, it

	GRPEL1	GRPEL2	GRPEL2-C87A	GRPEL2-C97A
Fit model	Kd	Kd	Kd	Kd
Bound	949.68	953.13	949.9	950.8
Unbound	936.37	936.75	934.4	934.9
Kd (nM)	<b>370</b>	<b>373</b>	<b>203</b>	<b>457</b>
Target conc (nM)	10	10	10	10
Standard deviation	0.62	0.5	0.47	0.64
Kd confidence	±6.2E-08	±4.03E-08	±2.04E-08	±4.4-08

**TABLE 4** MST fit information for the interaction of mtHSP70 (target) with the ligands GRPEL1, GRPEL2, GRPEL2-C87A, and GRPEL2-C97A.

*Note:* In non-reducing conditions, GRPEL1 exhibits similar affinity to mtHSP70 compared with GRPEL2 and GRPEL2-C97A. Notably, GRPEL2-C87A demonstrates the highest affinity among all ligands in this context. Bold represents the emphasis on the obtained experimental value which are crucial results.

is necessary to regulate and adapt the mitochondrial protein import machinery to match the cellular requirements (Baker et al., 2007). Earlier studies by us and others have suggested that GRPEL1 is the housekeeping NEF for mtHsp70 in mitochondrial matrix protein import (Konovalova et al., 2018; Neupane et al., 2022; Srivastava et al., 2017). In contrast, loss of GRPEL2 in cultured human cells did not affect protein import, but a role for GRPEL2 in oxidative stress was proposed (Konovalova et al., 2018). Despite the prominent structural resemblance of these two paralogs, we here demonstrate the biophysical and biochemical differences between human recombinant GRPELs, which support their functional roles.

The mtHSP70 cycle constantly transits from a high substrate affinity state (ADP bound) to a low substrate affinity state (ATP bound) (Clerico et al., 2019; Mayer & Gierasch, 2019). At the ADP bound state, NEF binds to the mtHSP70 NBD and facilitates release of ADP and exchanges to ATP (Bracher & Verghese, 2023; Mayer & Gierasch, 2019; Rossi et al., 2024). We observed that upon addition of ADP, the affinity between GRPEL1 and mtHSP70 increased ~approximately 20-fold, with a determined  $K_D$  value of 13.4 nM, which is even lower than that previously observed with bacterial GrpE and DnaK (Harrison et al., 1997; Srivastava et al., 2017). Conversely, with the addition of ADP, the affinity for GRPEL2 was nearly 100-fold lower, strongly indicating that the interaction between GRPEL1 and ADP-mtHSP70 is unequivocal and could be exclusive. Our functional Pi assay showed enhanced ATPase activity by mtHSP70 in the presence of GRPEL1. The reaction with mtHSP70 alone had a slow accumulation of free Pi over time showing the protein's intrinsic ATP hydrolysis, as also observed previously (Zhai et al., 2008). The reaction of mtHSP70 with GRPEL2 showed similar levels of Pi accumulation as mtHSP70 alone, indicating inability to enhance ATP hydrolysis. The differential capabilities of GRPEL1 and GRPEL2 were also supported by our ATPase activity

assay, contrasting with an earlier study that suggested NEF activity of both GRPEL1 and GRPEL2 (Srivastava et al., 2017).

In the recent cryo-EM structure of *M. tuberculosis* GrpE–DnaK, the preferential stoichiometry between prokaryotic GrpE and DnaK was shown as 2:1, while the 2:2 stoichiometry may hinder the NEF flexibility for the allosteric regulation of the chaperone (Xiao et al., 2024). Our SEC-MALS analysis showed that GRPEL1 forms two complexes with mtHSP70, with stoichiometries of 2:1 and 2:2, corroborating findings from the earlier crystallographic studies with bacterial GrpE–DnaK complexes (Harrison et al., 1997; Wu et al., 2012). Yet, our modeled complex favors 2:1 interaction for the functionality of GRPEL1. Previous studies of the *G. kaustophilus* GrpE–DnaK complex crystal structure and the *M. tuberculosis* GrpE–DnaK complex cryo-EM structure have revealed interactions between the GrpE homodimer's four-helical bundle region and DnaK's NBD (Wu et al., 2012; Xiao et al., 2024). This interaction, involving the  $\beta$ -hairpin structure near DnaK's NBD (region IIB), aids in ADP release from DnaK. In the *E. coli* GrpE–DnaK complex, this interaction is disrupted by the G122D point mutation (Harrison et al., 1997). However, recent AlphaFold modeling suggests that wild-type *E. coli* GrpE can open DnaK's NBD through similar interactions (Rossi et al., 2024). Our AlphaFold-based modeling suggests that GRPEL1 can interact with region IIB of the NBD of mtHSP70, opening its nucleotide-binding pocket. However, in our GRPEL2-NBD modeling, this interaction was absent, leaving the NBD pocket closed. This aligns with the results of our MST studies and the functional Pi assay, showing a significant loss of affinity in the presence of ADP in the GRPEL2-mtHSP70 mixture and no enhanced Pi accumulation. Additionally, SEC-MALS experiments revealed no complex formation between GRPEL2 and mtHSP70. Both GRPELs maintain a fully symmetric homodimeric structure in our calculated complexes, differing from GrpE–DnaK structures where GrpE

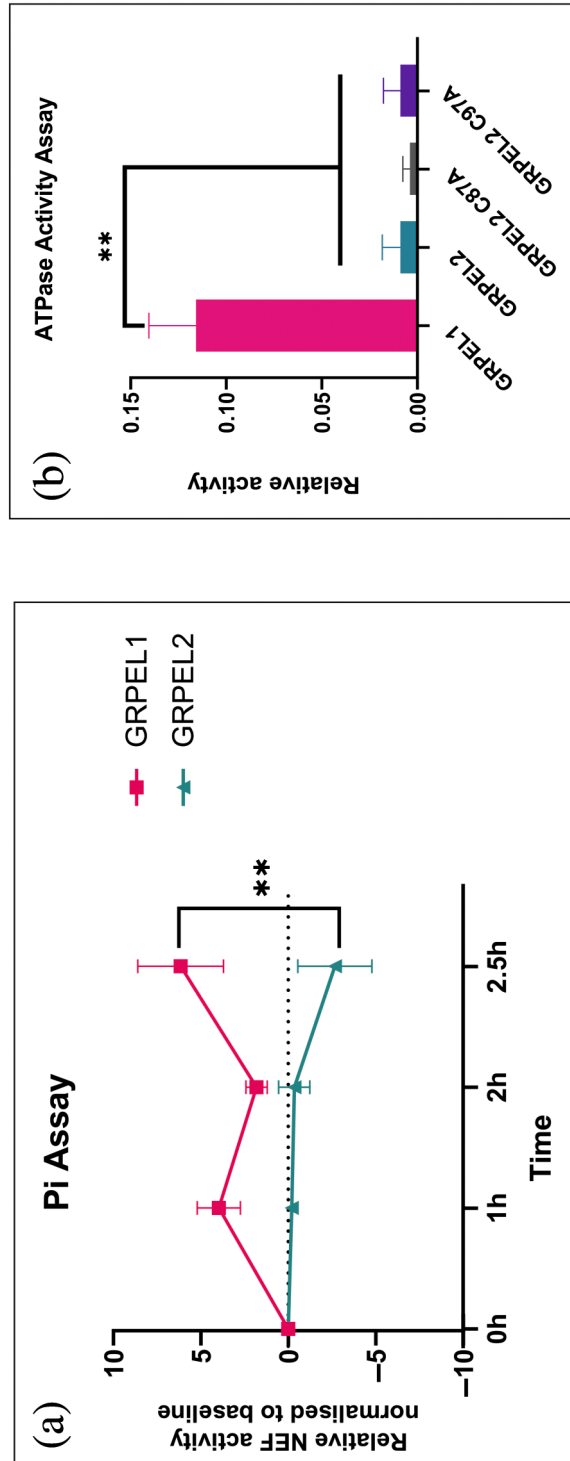


**FIGURE 7** NEF activity is enhanced by GRPEL1. The analysis of free inorganic phosphate obtained after ATP hydrolysis by mtHSP70 with or without GRPEL1 and GRPEL2. (a) Relative NEF activity of GRPEL1 and GRPEL2 normalized to baseline activity of mtHSP70 alone. The mean ( $\pm$ SD) was calculated from  $n = 3$  replicates, and the  $p < 0.0001$  was determined by two-way Anova. (b) NEF activity is shown through ATPase assay where the reaction contained a constant amount of mtHSP70 complexed with radiolabeled ATP. Relative NEF activity of GRPEL1 and GRPEL2. GRPEL2 C87A and GRPEL2 C97A in ATP hydrolysis by mtHSP70 was determined and normalized to ATPase activity of mtHSP70 alone. The mean ( $\pm$ SD) was calculated from  $n = 3$  replicates and statistical significance was determined by one-way ANOVA,  $p < 0.0001$ .

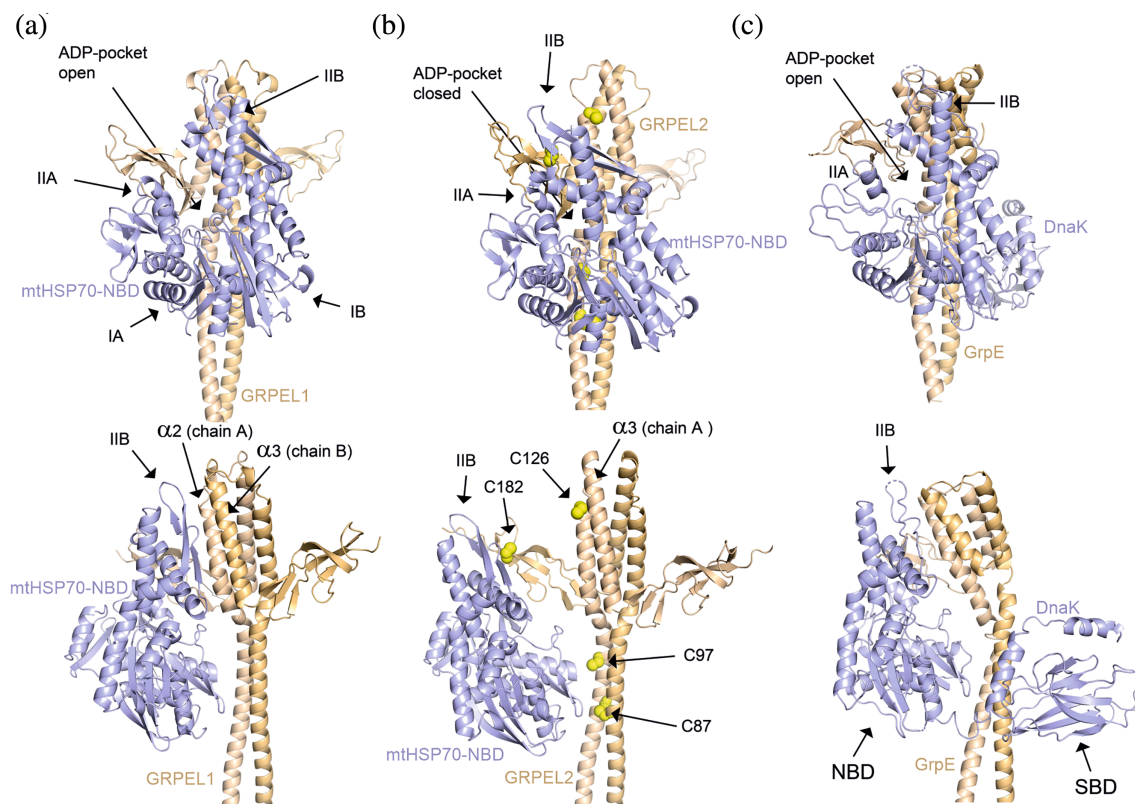


**FIGURE 8** The modeling studies of GRPEL1 and GRPEL2 with the nucleotide binding domain of mtHSP70. The AlphaFold model of homodimeric GRPEL1 (a) and GRPEL2 (b) complexed with NBD of mtHSP70 shown with two different views. The top view provides a clearer depiction of the open and closed conformations of the NBD of HSP70, while the bottom view offers a more detailed representation of the GRPEL dimer and its interaction sites with the chaperone. The two chains of the GRPEL homodimers are colored light brown and orange, and the NBD of mtHSP70 in blue. In the case of GRPEL2, it also highlights the critical cysteines. (c) Cryo-EM structure of Tb GrpE (light brown and orange) and the bound DnaK (blue). The NBD and SBD are labeled. NBD contains four subdomain regions referred to as IA, IIA, IB, and IIB. The nucleotide-binding pocket is formed in between subdomains IIA and IIB as shown in the figure. The four-helical bundle region, formed by helices  $\alpha 2$  and  $\alpha 2$ , are heavily interacting with the subdomain IIB of NBD facilitating the fully open nucleotide-binding pocket in the *M. tuberculosis* GrpE–DnaK structure (panel c). This critical interaction is also seen in the modeled complex structure of GRPEL1 and NBD (panel a), whereas in the modeled complex of GRPEL2–NBD, this interaction is not seen at all (panel c).

curves toward the NBD (Wu et al., 2012; Xiao et al., 2024). We hypothesize that the C87–C87 disulfide bridge in GRPEL2's coiled-coil region renders its homodimer too rigid for bending, hindering interaction with mtHSP70. Differences in amino acid sequences in  $\alpha$ -helices  $\alpha 2$  and  $\alpha 3$  may also reduce GRPEL2's affinity with NBD region IIB, particularly in its ADP-bound conformation requiring coiled-coil flexibility.

We earlier showed that oxidative stress induced by hydrogen peroxide in cultured human cells increased GRPEL2 dimer formation, a phenomenon contingent upon Cys87 (Konovalova et al., 2018), a cysteine unique to GRPEL2. On the contrary, in yeast, Mge1 Met155 responds to oxidative stress, enhancing monomers (Marada et al., 2013). Based on our findings in the present study, we propose that the Cys87 disulfide bridge is not critical for GRPEL2 dimerization in an aqueous solution. The findings from SEC-MALS analysis validate that

both the C87A and C97A mutants of GRPEL2 exhibit a behavior alike to the wild type, predominantly existing as dimers with a minority of tetramers. This suggests that the presence or absence of Cys residues does not significantly affect the quaternary structures of the protein. Moreover, we postulate that under conditions of oxidative stress, Cys87 plays a role in stabilizing the long alpha helix within GRPEL2, potentially improving the protein's overall functionality during stress. However, a comprehensive exploration of this phenomenon is warranted to elucidate its full implications.

Disulfide bonds and protein dimerization are known to notably enhance the stability of secondary structures (Betz, 1993; Fass, 2012). The GRPELs showed a preferred oligomeric state of dimers and a low number of tetramers in the SEC-MALS analysis. These higher-order oligomeric states likely contribute to enhanced stability of the secondary structure. This was corroborated by CD

spectra, confirming proper protein folding and functionality. Notably, GRPEL1 exhibited greater thermal stability compared to GRPEL2 in non-reduced buffer, consistent with previous findings (Borges et al., 2003; Oliveira et al., 2006). However, mutations in GRPEL2 (C87A and C97A) resulted in improved stability under non-reducing conditions. This can be attributed to the prevention of non-functional disulfide bonds, thus preserving the native protein structure (Karimi et al., 2016). Moreover, GRPEL1 showed enhanced thermal stability under reduced conditions, where the conformation becomes more flexible and less constrained, as suggested by earlier studies (Creighton, 1988). Overall, these observations suggest that GRPEL1 in reduced conformation exhibit increased stability and improved resistance to aggregation. Our MST studies analysis showed that both GRPELs had better affinity under reduced conditions. The affinity between GRPEL2-C97A and mtHSP70 was closer to that of wild-type GRPEL2 in the non-reduced form. Notably, the GRPEL2-C87A variant, with a  $K_D$  of 204 nM, was comparable with the  $K_D$  of 152 nM between wild type GRPEL2 and mtHSP70 in the presence of DTT. This implies that the Cys87 disulfide bond of the GRPEL2 dimer reduces GRPEL2 interaction with mtHSP70.

The remaining cysteines were not investigated in this study; nevertheless, there is a possibility that they contribute to redox sensing. Specifically, Cys126 and Cys182 warrant further exploration to understand their potential redox-regulatory roles. Our model and known GrpE-DnaK structures indicate that both cysteines reside in a region conducive to protein-protein interactions. Notably, Cys182 is exclusive to GRPEL2. In GRPEL2, when all six cysteines are reduced, wild-type and mutants show similar structures and stability, indicating Cys87 and Cys97 significantly impact GRPEL2 stability and function. These findings hint that if GRPEL2 functions as a redox sensor, it stabilizes by forming disulfide bonds to an already existing dimer. It is conceivable that the rigidity of the coiled-coil helices plays a crucial role in this context.

The chaperones such as mtHSP70 are susceptible to constant allosteric changes where NEFs and the substrate protein impact chaperone's structure (Li et al., 2016). A prior study revealed that a network mediated by  $Mg^{2+}$  ions effectively enhanced the affinity of human recombinant mtHSP70 for ADP. Interestingly, NEFs were found to systematically dismantle this network, leading to a gradual release of ADP and creating conditions conducive for ATP binding (Arakawa et al., 2011). Similarly, ADP-bound mtHSP70 may exhibit a conformational change, establishing a distinct preference solely for GRPEL1. Post-translational modifications are known to modulate the interaction dynamics of chaperones, as demonstrated by recent findings regarding the acetylation of specific lysine

residues in mtHSP70 (Gao et al., 2024). Similarly, ADP may employ a crucial influence on the selection of the co-chaperone for mtHSP70 by inducing conformational changes in the chaperone protein. This intricate interplay between nucleotide binding, post-translational modifications, and co-chaperone selection highlights the sophisticated regulatory mechanisms governing the intricate protein folding processes within the mitochondrial matrix.

In summary, our study illustrates the distinct binding preferences between ADP-mtHSP70 and GRPEL1, highlighting GRPEL1 as the primary co-chaperone for mtHSP70. Conversely, the presence of disulfide bonds in GRPEL2 appears to diminish its affinity for ADP-bound mtHSP70, thereby favoring GRPEL1 for functional interactions. Although GRPEL2 predominantly adopts an oligomeric state facilitated by disulfide formation, this process may impose rigidity on the alpha helix, compromising its stability and affinity for mtHSP70. These insights shed light on the contrasting roles of GRPEL1 and GRPEL2 in human cells, providing structural clarity in their functional distinctions.

## 4 | MATERIALS AND METHODS

### 4.1 | Cloning and protein purification

The GRPEL constructs (contain no mitochondrial targeting sequence and presence of TEV cleavage site) encoding full-length GRPEL1, GRPEL2, GRPEL2-C87A, and GRPEL2-C97A were generated by PCR amplification using a forward primer containing the NcoI site and a reverse primer containing the Acco65I site followed by a STOP codon (TAA) (Table S2). The amplified product was digested using NcoI and Acco65I and ligated into a linear (double digested) pETHis1a (+) plasmid. The resulting sequences were verified by Sanger sequencing. The mtHSP70 was expressed from a pRSFDuet-1 plasmid coding for human mtHSP70 and yeast Zim17 and was kind gift of Professor Patrick D'Silva (Department of Biochemistry, Indian Institute of Science, Bangalore, India).

Proteins were expressed in BL21(DE3) strain and grown overnight at 37°C. Secondary cultures reached an OD of 0.6 at 30°C before induction with 0.5 mM IPTG for 12 h. Cells were collected by centrifugation at 4000g for 10 min at 4°C, then lysed in 150 mM Tris pH 8, 200 mM NaCl, 5% glycerol, 50 mM imidazole with 0.5 mg/mL lysozyme, and incubated for 45 min at 4°C followed by 0.2% DOC for 15 min at 4°C. The lysate was centrifuged at 18000g for 30 min at 4°C. Ni-NTA beads were incubated with the supernatant at 4°C for 1 h. Unbound proteins were collected in the flow-through, and elution was performed with 8 elutions of 1 mL each

using elution buffer: 150 mM Tris pH 8, 200 mM NaCl, 5% glycerol, and 250 mM imidazole.

## 4.2 | Size exclusion chromatography (SEC)

Gel filtration was performed using concentrated IMAC purified proteins of 500  $\mu$ L in volume using a Superdex 75 GL column and Superdex-200 10/300 GL column preparative grade size exclusion chromatography column (GE Healthcare). The column was pre-equilibrated with SEC buffer composed of 50 mM Tris-HCl, 50 mM NaCl, 100 mM imidazole, and 5% glycerol at pH 8.0. The final protein solution was concentrated at  $\sim$ 5–6 mg/mL (concentration was measured using BCA) and stored in SEC buffer in 50 L aliquot volumes at  $-80^{\circ}\text{C}$ .

## 4.3 | SDS-PAGE

For reducing/non-reducing SDS-PAGE, sample buffer for non-reducing (250 mM Tris-HCl (pH 6.8), 10% SDS, 30% glycerol, 0.02% bromophenol blue) and reducing (Laemmli sample buffer (Bio-Rad) including 10%  $\beta$ -mercaptoethanol) conditions were used. Proteins for reducing SDS-PAGE were boiled at  $95^{\circ}\text{C}$  for 10 min and spun before loading. For clear native PAGE, the sample buffer was 62.5 mM Tris-HCl, pH 6.8, 25% (v/v) glycerol, 0.01% (w/v) bromophenol blue, and the running buffer was 25 mM Tris and 192 mM glycine.

## 4.4 | Static light scattering (SLS)

MALS analyses of all the GRPELs and mtHSP70 were carried out using the miniDAWN<sup>TM</sup> MALS detector (Wyatt Technologies). For these experiments, 50–100  $\mu$ L of the purified protein samples (concentration ranging 2–15 mg/mL) were filtered (with 0.1  $\mu$ m pore size) and loaded onto a Superdex200 10/300GL column (GE Healthcare) preequilibrated with SEC buffer. Before entering the MALS detector, the samples flow through a Optilab refractive index (RI) detector (Wyatt Technologies). The RI signal is used to measure the concentration of the protein sample. Molecular mass, polydispersity, and other analyses were carried out using the ASTRA software (Wyatt Technologies).

## 4.5 | Circular dichroism (CD) spectroscopy

Circular dichroism (CD) spectroscopy was performed using a Chirascan CD spectrometer (Applied Photophysics,

Leatherhead, UK). CD data were collected between 280 and 190 nm at  $22^{\circ}\text{C}$  using a 0.1-cm path-length quartz cuvette. CD measurements were acquired every 1 nm with 0.5 s as the integration time and repeated three times with baseline correction. Data were processed using the Chirascan Pro-Data Viewer (Applied Photophysics) and CDNN (<http://www.xn-gerald-bhm-lcb.de/download/cdmn>). Direct CD measurements ( $\theta$ ; mdeg) were converted into mean residue molar ellipticity ( $[\theta]_{\text{MR}}$ ) by Pro-Data Viewer. The  $T_m$  was measured with a temperature ramping from 22 to  $72^{\circ}\text{C}$  at a rate of  $1^{\circ}\text{C}/\text{min}$ . The data were analyzed using Global 3 (Applied Photophysics). Purified GRPEL1, GRPEL2, GRPEL2-C87A, and GRPEL2-C97A proteins were first diluted to 2.7 mg/mL in the  $1\times$  buffer (50 mM Tris pH 8, 100 mM NaCl, 100 mM imidazole, 5% glycerol) and then 1:54 diluted in  $\text{dH}_2\text{O}$ . The final solution buffer was 0.93 mM Tris pH 8, 1.85 mM NaCl, 1.85 mM imidazole, 1.9% glycerol. All samples were treated with 1 mM DTT. The final solution buffer was 0.93 mM Tris pH 8, 1.85 mM NaCl, 1.85 mM imidazole, 1.9% glycerol, 1 mM DTT. The final concentrations were verified by measuring the absorbance of the protein solution at 214 or 205 nm. For statistical analysis, three independent runs were considered, and GraphPad Prism 2way-ANOVA was used for comparisons.

## 4.6 | Microscale thermophoresis (MST)

MST was performed using Nanotemper Monolith NT.115. Proteins were labeled with a second-generation red-tris-NTA NT-650-NHS fluorescent dye using a Nanotemper labelling kit (MO-L011). The mtHSP70 to HIS-tag fluorescent dye concentration ratio was 1:1 and incubated at room temperature for 30 min. Excess dye was removed by centrifugation for 10 min at  $4^{\circ}\text{C}$  and 15,000g. The actual protein concentration was determined using a NanoDrop microvolume spectrophotometer after correcting for the extinction coefficient of the proteins. Binding experiments were performed in PBS-Tween-20 buffer (10 mM PBS, 150 mM NaCl, 0.05% Tween-20, pH 8). The binding assays were performed with a fixed concentration (10 nM) of fluorescently labeled mtHSP70 (monomer) and twofold serially diluted decreasing concentrations of unlabeled (dimeric form was considered for the concentration of GRPELs) GRPEL1, GRPEL2, GRPEL2-C87A, and GRPEL2-C97A (all the GRPELs' His-tags were cleaved at TEV-cleavage site and buffer exchange to MST buffer was performed). The reaction mixture of 16 serial diluents of the ligand and labeled protein was filled into the capillary tubes (Nanotemper, MO-K022) and loaded in the Monolith NT.115 instrument accordingly. The MST buffer used contained 1 mM DTT and 1 mM ADP as per the

requirement of the experimental set up. All experiments were performed at 25°C using a medium MST power and 20% LED power. In MST, “bound” (refers to the state where the target molecule is interacting with a ligand or binding partner) and “unbound” (refers to the state where the target molecule is free and not interacting with the ligand) states differentiate the interaction between molecules, enabling the measurement of binding affinity. Analysis was conducted using 1.5 s MST power on and three independent experiments were considered of mean SD calculation and MST traces are shown in the supplementary information (Figure S8).

#### 4.7 | Nucleotide exchange factor activity assay (Pi assay)

To assess nucleotide exchange factor (NEF) activity, we utilized a malachite green dye and molybdate assay, following the method described previously (Geladopoulos et al., 1991), which capitalizes on inorganic phosphate (Pi) forming a complex with malachite green dye mixture, showing absorbance at 625 nm. This complex is specific for Pi released after ATP hydrolysis by mtHSP70. Our experimental setup included a baseline reaction with 6  $\mu$ M mtHSP70 (monomer) and 600  $\mu$ M ATP, and two test reactions with 6  $\mu$ M of either GRPEL1 or GRPEL2 (dimeric form was considered for calculations) along with 600  $\mu$ M ATP. The blank reaction contained only buffer with ATP. Each reaction mixture, containing 50 mM Tris-HCl (pH 7), proteins, and ATP, was prepared in a total volume of 20  $\mu$ L. Incubations were carried out at 37°C for four different time points: 0, 1 h, 2 h, and 2 h 30 min. Following incubation, ultra-pure water (Sigma) was added to bring the volume to 80  $\mu$ L, and the mixtures were transferred to SpectraPlate™-96MB microplates (PerkinElmer #6055649). A 20  $\mu$ L volume of malachite green mix (7.5% ammonium molybdate, 0.33 mM malachite green, 20% Tween-20) was added, mixed well, and incubated at room temperature for 5 min. Pi concentrations were evaluated using phosphate standards (Na<sub>2</sub>HPO<sub>4</sub>) at 10, 25, 50, and 70  $\mu$ M, and a buffer-only blank. Absorbance readings at 625 nm were taken with a plate reader, and the data were analyzed using GraphPad Prism with statistical significance evaluated via one-way ANOVA.

#### 4.8 | ATPase assay

In the mtHsp70 ATPase assay, 50  $\mu$ g of mtHsp70 protein was incubated with 25  $\mu$ Ci of [ $\gamma$ -<sup>32</sup>P] ATP in 50  $\mu$ L of Buffer X (25 mM HEPES-KOH, pH 7.5, 100 mM KCl,

10 mM magnesium acetate) for 3 min on ice. The reaction mixture was then purified using a G-25 column pre-equilibrated with Buffer A (25 mM HEPES-KOH, pH 7.5, 100 mM KCl, 10 mM magnesium acetate, 20 mM imidazole), and glycerol was added to the purified mixture to a final concentration of 10%. For single turnover experiments, the reaction was prepared in Buffer A containing 0.4  $\mu$ M mtHsp70 and 10  $\mu$ M cold ATP, with or without the presence of GrpEL1/2 proteins (1.4  $\mu$ M). The reaction components were mixed, incubated on ice for 10 min, and then further incubated at 37°C for 30 min. The reaction was stopped by adding 4 $\times$  Laemmli buffer, and the samples were separated by electrophoresis on a 12% TBE gel at 100 V for 20 min. The gels were then dried, imaged using an Amersham Typhoon phosphor imager, and analyzed with ImageJ software. For analysis, relative activity was determined by normalizing the mtHSP70-ATP alone and statistical calculation of three assays was determined by one-way ANOVA using GraphPad Prism.

#### 4.9 | Modeling calculations

The homodimeric models of GRPEL1 and GRPEL2 were generated using an AlphaFold Colab notebook (Jumper et al., 2021). The heterocomplex models of GRPEL1 or GRPEL2 with mtHSP70 were calculated using AlphaFold-multimer (Evans et al., 2021) in the COSMIC2 cloud platform for structural biology research and education (Cianfrocco et al., n.d.).

#### AUTHOR CONTRIBUTIONS

**Pooja Manjunath:** Conceptualization; methodology; validation; writing – review and editing; writing – original draft; investigation. **Gorazd Stojkovič:** Conceptualization; methodology; writing – review and editing. **Liliya Euro:** Methodology; supervision; visualization. **Svetlana Konovalova:** Conceptualization; investigation; writing – review and editing. **Sjoerd Wanrooij:** Conceptualization; writing – review and editing; supervision. **Kristian Koski:** Conceptualization; investigation; methodology; writing – review and editing; writing – original draft. **Henna Tyynismaa:** Conceptualization; investigation; funding acquisition; writing – original draft; writing – review and editing; supervision.

#### ACKNOWLEDGMENTS

Riitta Lehtinen, Miia Nissilä, and Jana Pennonen are acknowledged for their technical support. The facilities and expertise of the BCO Structural Biology and Molecular Biophysics core (especially Dr. Hongmin Tu), all the members of Biocenter Finland, INSTRUCT-ERIC Centre Finland, and FINStruct are gratefully

acknowledged. This work benefited the access to the BCO and Instruct-ERIC center with the financial support provided by Instruct-ERIC (PID:9479). The authors thank the funding support from the Academy of Finland Centre of Excellence (MetaStem), the Sigrid Juselius Foundation (for HT), and the Orion Foundation (for PM).

## CONFLICT OF INTEREST STATEMENT

The authors declare no conflicts of interest.

## ORCID

Pooja Manjunath  <https://orcid.org/0000-0002-9449-6443>

Gorazd Stojkovič  <https://orcid.org/0000-0003-0651-9666>

## REFERENCES

- Arakawa A, Handa N, Shirouzu M, Yokoyama S. Biochemical and structural studies on the high affinity of Hsp70 for ADP. *Protein Sci.* 2011;20:1367–79.
- Baker MJ, Frazier AE, Gulbis JM, Ryan MT. Mitochondrial protein-import machinery: correlating structure with function. *Trends Cell Biol.* 2007;17:456–64.
- Betz SF. Disulfide bonds and the stability of globular proteins. *Protein Sci.* 1993;2:1551–8.
- Bolliger L, Deloche O, Glick BS, Georgopoulos C, Jenö P, Kronidou N, et al. A mitochondrial homolog of bacterial GrpE interacts with mitochondrial hsp70 and is essential for viability. *EMBO J.* 1994;13:1998–2006.
- Borges JC, Fischer H, Craievich AF, Hansen LD, Ramos CH. Free human mitochondrial GrpE is a symmetric dimer in solution. *J Biol Chem.* 2003;278:35337–44.
- Bracher A, Verghese J. Nucleotide exchange factors for Hsp70 molecular chaperones: GrpE, Hsp110/Grp170, HspBP1/Sil1, and BAG domain proteins. *Subcell Biochem.* 2023;101:1–39.
- Cianfrocco MA, Wong-Barnum M, Youn C, Wagner R, Leschziner A. COSMIC2. *ACM.*
- Clerico EM, Meng W, Pozhidaeva A, Bhasne K, Petridis C, Gierasch LM. Hsp70 molecular chaperones: multifunctional allosteric holding and unfolding machines. *Biochem J.* 2019;476:1653–77.
- Creighton TE. Disulphide bonds and protein stability. *BioEssays.* 1988;8:57–63.
- Evans R, O'Neill M, Pritzel A, Antropova N, Senior A, Green T, et al. Protein complex prediction with AlphaFold-multimer. Cold Spring Harbor Laboratory; 2021.
- Fass D. Disulfide bonding in protein biophysics. *Annu Rev Biophys.* 2012;41:63–79.
- Gao B, Wang Z, Dai K, Wang Y, Li L, Li G, et al. Acetylation of mtHSP70 at Lys595/653 affecting its interaction between GrpEL1 regulates glioblastoma progression via UPRmt. *Free Radic Biol Med.* 2024;213:394–408.
- Geladopoulos TP, Sotiroidis TG, Evangelopoulos AE. A malachite green colorimetric assay for protein phosphatase activity. *Anal Biochem.* 1991;192:112–6.
- Goswami AV, Chittoor B, D'Silva P. Understanding the functional interplay between mammalian mitochondrial Hsp70 chaperone machine components. *J Biol Chem.* 2010;285:19472–82.
- Grimshaw JP, Siegenthaler RK, Zuger S, Schonfeld HJ, Z'Graggen BR, Christen P. The heat-sensitive *Escherichia coli* grpE280 phenotype: impaired interaction of GrpE(G122D) with DnaK. *J Mol Biol.* 2005;353:888–96.
- Harrison C. GrpE, a nucleotide exchange factor for DnaK. *Cell Stress Chaperones.* 2003;8:218–24.
- Harrison CJ, Hayer-Hartl M, Di Liberto M, Hartl F, Kuriyan J. Crystal structure of the nucleotide exchange factor GrpE bound to the ATPase domain of the molecular chaperone DnaK. *Science.* 1997;276:431–5.
- Hosfelt J, Richards A, Zheng M, Adura C, Nelson B, Yang A, et al. An allosteric inhibitor of bacterial Hsp70 chaperone potentiates antibiotics and mitigates resistance. *Cell Chem Biol.* 2022;29:854–69.
- Jumper J, Evans R, Pritzel A, Green T, Figurnov M, Ronneberger O, et al. Highly accurate protein structure prediction with AlphaFold. *Nature.* 2021;596:583–9.
- Kang PJ, Ostermann J, Shilling J, Neupert W, Craig EA, Pfanner N. Requirement for hsp70 in the mitochondrial matrix for translocation and folding of precursor proteins. *Nature.* 1990;348:137–43.
- Karimi M, Ignasiak MT, Chan B, Croft AK, Radom L, Schiesser CH, et al. Reactivity of disulfide bonds is markedly affected by structure and environment: implications for protein modification and stability. *Sci Rep.* 2016;6:38572.
- Kisty EA, Saart EC, Weerapana E. Identifying redox-sensitive cysteine residues in mitochondria. *Antioxidants.* 2023;12(5):992.
- Konovalova S, Liu X, Manjunath P, Baral S, Neupane N, Hilander T, et al. Redox regulation of GRPEL2 nucleotide exchange factor for mitochondrial HSP70 chaperone. *Redox Biol.* 2018;19:37–45.
- Krzewska J, Langer T, Liberek K. Mitochondrial Hsp78, a member of the Clp/Hsp100 family in *Saccharomyces cerevisiae*, cooperates with Hsp70 in protein refolding. *FEBS Lett.* 2001;489:92–6.
- Laloraya S, Gambill BD, Craig EA. A role for a eukaryotic GrpE-related protein, Mge1p, in protein translocation. *Proc Natl Acad Sci USA.* 1994;91:6481–5.
- Li X, Shao H, Taylor IR, Gestwicki JE. Targeting allosteric control mechanisms in heat shock protein 70 (Hsp70). *Curr Top Med Chem.* 2016;16:2729–40.
- Liberek K, Marszałek J, Ang D, Georgopoulos C, Zylicz M. *Escherichia coli* DnaJ and GrpE heat shock proteins jointly stimulate ATPase activity of DnaK. *Proc Natl Acad Sci USA.* 1991;88:2874–8.
- Marada A, Allu PK, Murari A, PullaReddy B, Tammineni P, Thiriveedi VR, et al. Mge1, a nucleotide exchange factor of Hsp70, acts as an oxidative sensor to regulate mitochondrial Hsp70 function. *Mol Biol Cell.* 2013;24:692–703.
- Mayer MP, Gierasch LM. Recent advances in the structural and mechanistic aspects of Hsp70 molecular chaperones. *J Biol Chem.* 2019;294:2085–97.
- Moro F, Muga A. Thermal adaptation of the yeast mitochondrial Hsp70 system is regulated by the reversible unfolding of its nucleotide exchange factor. *J Mol Biol.* 2006;358:1367–77.
- Nakamura A, Takumi K, Miki K. Crystal structure of a thermophilic GrpE protein: insight into thermosensing function for the DnaK chaperone system. *J Mol Biol.* 2010;396:1000–11.
- Naylor DJ, Hoogenraad NJ, Hoj PB. Isolation and characterisation of a cDNA encoding rat mitochondrial GrpE, a stress-inducible



- nucleotide-exchange factor of ubiquitous appearance in mammalian organs. *FEBS Lett.* 1996;396:181–8.
- Naylor DJ, Stines AP, Hoogenraad NJ, Hoj PB. Evidence for the existence of distinct mammalian cytosolic, microsomal, and two mitochondrial GrpE-like proteins, the Co-chaperones of specific Hsp70 members. *J Biol Chem.* 1998;273:21169–77.
- Neupane N, Rajendran J, Kvist J, Harjuhaahto S, Hu B, Kinnunen V, et al. Inter-organellar and systemic responses to impaired mitochondrial matrix protein import in skeletal muscle. *Commun Biol.* 2022;5:1060.
- Oliveira CL, Borges JC, Torriani IL, Ramos CH. Low resolution structure and stability studies of human GrpE#2, a mitochondrial nucleotide exchange factor. *Arch Biochem Biophys.* 2006;449:77–86.
- Rossi MA, Pozhidaeva AK, Clerico EM, Petridis C, Gierasch LM. New insights into the structure and function of the complex between the *Escherichia coli* Hsp70, DnaK, and its nucleotide-exchange factor, GrpE. *J Biol Chem.* 2024;300:105574.
- Srivastava S, Savanur MA, Sinha D, Birje A, Vigneshwaran R, Saha PP, et al. Regulation of mitochondrial protein import by the nucleotide exchange factors GrpEL1 and GrpEL2 in human cells. *J Biol Chem.* 2017;292:18075–90.
- Szabo A, Langer T, Schroder H, Flanagan J, Bukau B, Hartl FU. The ATP hydrolysis-dependent reaction cycle of the *Escherichia coli* Hsp70 system DnaK, DnaJ, and GrpE. *Proc Natl Acad Sci USA.* 1994;91:10345–9.
- Wu CC, Naveen V, Chien CH, Chang YW, Hsiao CD. Crystal structure of DnaK protein complexed with nucleotide exchange factor GrpE in DnaK chaperone system: insight into intermolecular communication. *J Biol Chem.* 2012;287:21461–70.
- Xiao X, Fay A, Molina PS, Kovach A, Glickman MS, Li H. Structure of the *M. tuberculosis* DnaK-GrpE complex reveals how key DnaK roles are controlled. *Nat Commun.* 2024;15:660.
- Zhai P, Stanworth C, Liu S, Silberg JJ. The human escort protein hep binds to the ATPase domain of mitochondrial hsp70 and regulates ATP hydrolysis. *J Biol Chem.* 2008;283:26098–106.

## SUPPORTING INFORMATION

Additional supporting information can be found online in the Supporting Information section at the end of this article.

**How to cite this article:** Manjunath P, Stojkovič G, Euro L, Konovalova S, Wanrooij S, Koski K, et al. Preferential binding of ADP-bound mitochondrial HSP70 to the nucleotide exchange factor GRPEL1 over GRPEL2. *Protein Science.* 2024;33(11):e5190. <https://doi.org/10.1002/pro.5190>